

## Laser Implosion of High-Aspect-Ratio Targets Produces Thermonuclear Neutron Yields Exceeding $10^{12}$ by Use of Shock Multiplexing

C. Yamanaka, S. Nakai, T. Yabe, H. Nishimura, S. Uchida, Y. Izawa, T. Norimatsu, N. Miyanaga, H. Azechi, M. Nakai, H. Takabe, J. Jitsuno, K. Mima, M. Nakatsuka, T. Sasaki, M. Yamanaka, Y. Kato, T. Mochizuki, Y. Kitagawa, T. Yamanaka, and K. Yoshida

*Institute of Laser Engineering, Osaka University, Yamada-Oka, Suita, Osaka 565, Japan*

(Received 25 November 1985)

Neutron yields in excess of  $10^{12}$  were achieved with the twelve-beam green GEKKO XII laser by choice of a shock-multiplexing implosion mode as predicted by a simulation code HIMICO. The first half of a Gaussian pulse was used to achieve a tailored implosion with shock multiplexing. The implosion mode is sensitive to the matching between the implosion time and the laser pulse. The simulation result suggests that the compression with a large deceleration at the stagnation phase due to the shock-wave multiplexing plays an important role in attainment of high neutron yields without pusher-fuel mixing in high-aspect-ratio D-T shell targets.

PACS numbers: 52.50.Jm, 52.55.Pi, 52.65.+z

Directly driven implosion has been extensively studied in the wake of the completion of short-wavelength laser systems.<sup>1-3</sup> In a long-wavelength laser, such as 1  $\mu\text{m}$ , hot electrons play a significant role in the energy transport by preheating the fuel and exploding the pusher. In a short-wavelength laser, however, the energy transport is conducted mainly by thermal electrons, which ablate the outer surface of a pusher, generating a high pressure ( $> 20$  Mbar) to drive the residual pusher and fuel inward.

As has long been pointed out, this ablative implosion may suffer from the Rayleigh-Taylor instability and the optimum aspect ratio acceptable in a target has been a subject of a considerable debate. In this Letter, we report experiments of direct implosion using the twelve-beam green GEKKO XII laser system.<sup>4</sup> By careful choice of the implosion mode as predicted by computer simulation, neutron production in excess of  $10^{12}$  was achieved. In the sense that the mode is close to a tailored ablative implosion,<sup>5</sup> the result represents a significant milestone in the inertial-confinement-fusion (ICF) research.

Two types of experiments were performed in order to clarify the implosion dynamics. In the first experiment (EXP-A), the laser output at 0.53- $\mu\text{m}$  wavelength was 0.9 TW in 800 psec FWHM, and the target was a glass microballoon (GMB) 545  $\mu\text{m}$  in diameter and 1.82  $\mu\text{m}$  thick coated with 3.6- $\mu\text{m}$ -thick CH and filled with 3.6 atm DT and 0.02 atm Ar. In the second experiment (EXP-B), the outputs at 0.53  $\mu\text{m}$  were 7.0–12.8 TW in 500 psec for targets  $500 \pm 20$   $\mu\text{m}$  and  $730 \pm 40$   $\mu\text{m}$  in diameter, and 6.4–10 TW in 750 psec for targets  $950 \pm 30$   $\mu\text{m}$  in diameter; the targets were DT-filled glass microballoons with aspect ratios ( $R/\Delta R$ , where  $\Delta R$  is the wall thickness) of 110–420, and gas pressures were from 3 to 13 atm with 0.02 atm of Ar gas. The energy balance among the beams was within 5% deviation. The targets were dodecahedrally irradiated with  $f/3$  lenses under a focusing condition

of  $d/R = -5$ , where  $d$  is the displacement of the focal point from the target center and  $R$  is the target radius. The focal position was set beyond the target center. The sphericity and wall uniformity of the targets were better than 1% and 5%, respectively. The target stem was less than 7  $\mu\text{m}$  in diameter to improve the heating uniformity.

Over 25 different diagnostics<sup>6</sup> were simultaneously used in the experiments to measure absorption, implosion dynamics, implosion uniformity, neutron yield, fuel temperature, fuel density  $\rho$ , and compression ratio. The time fiducial to the laser peak on the x-ray streak images was determined by independent laser shots using short-duration pulses. The possible errors were within  $\pm 70$  psec.

The top panels in Figs. 1(a) and 1(b) show x-ray streak images from the targets in EXP-A and EXP-B, respectively. These results were replicated by a one-dimensional simulation code, HIMICO,<sup>7</sup> which employs the non-local-thermodynamic-equilibrium average-ion model, multigroup radiation and electron transport, and a three-dimensional ray trace.<sup>8</sup> The flow diagram obtained by this code, with a flux limitation  $f_c = 0.03$  on the thermal electrons being incorporated with a nonlocal treatment, is given in the middle panels along with the time evolution of the time-integrated neutron yield; the positions of the x-ray peak intensity derived from the streak data are denoted by closed circles as a reference. The bottom panels display the time evolution of the pusher and fuel  $\rho R$ .

It should be noted in Fig. 1(a) that a reflected shock wave was clearly observed and also that the time history of the neutron yield  $N$  shows a shelf during the compression phase. This shelf is due to  $dN/dt$  having two peaks corresponding to neutrons from shock heating and from a further adiabatic compression. The absorption rate, ion temperature, implosion time, neutron yield, and implosion velocity were compared between the experiment and the simulation and it was

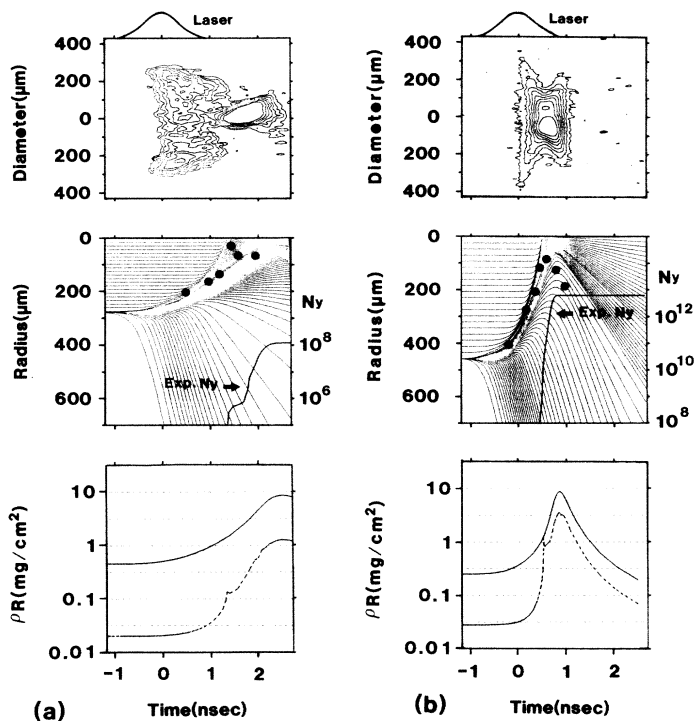


FIG. 1. (Bottom) Time evolution of  $\rho R$ , where the solid and the dashed lines represent the  $\rho R$  of the pusher and the fuel, respectively. (Middle) Flow diagrams and time-integrated neutron yields obtained by computer simulations. The experimental neutron yields are indicated by arrows. (Top) Isointensity contours of x-ray streak images of corresponding target shots. (a) 3.6-atm-DT-filled GMB of 545  $\mu\text{m}$  diam, 1.82  $\mu\text{m}$  thickness, coated with 3.6- $\mu\text{m}$ -thick CH, irradiated by 756 J per 800 psec at 0.53  $\mu\text{m}$  (EXP-A). (b) 3.0-atm-DT-filled GMB of 911  $\mu\text{m}$  diam, 1.46  $\mu\text{m}$  thickness, irradiated by 8045 J per 750 psec at 0.53  $\mu\text{m}$  (EXP-B).

found that all of the data could be consistently replicated with  $f_c$  between 0.03 and 0.04. It is important to point out that the neutron yield in the experiment is close to the value at this shelf. This tendency was common to identical shots. This result implies an important physical process; it was pointed out by Freeman, Clauser, and Thompson that the Rayleigh-Taylor instability with a high mode number may occur at the deceleration phase<sup>9,10</sup> and degrade the neutron production.

The result in Fig. 1(a) persuaded us to try a different implosion mode, an implosion mode in which the neutron yield occurs in one peak to achieve the highest neutron yield. Related to this mode, implosion with a tailored pulse has been a subject of considerable interest in ICF research. This mode utilizes shock-wave multiplexing<sup>5,11</sup>; all shock waves generated at different times collapse simultaneously at the center. On this basis, we found that a very thin-shell,

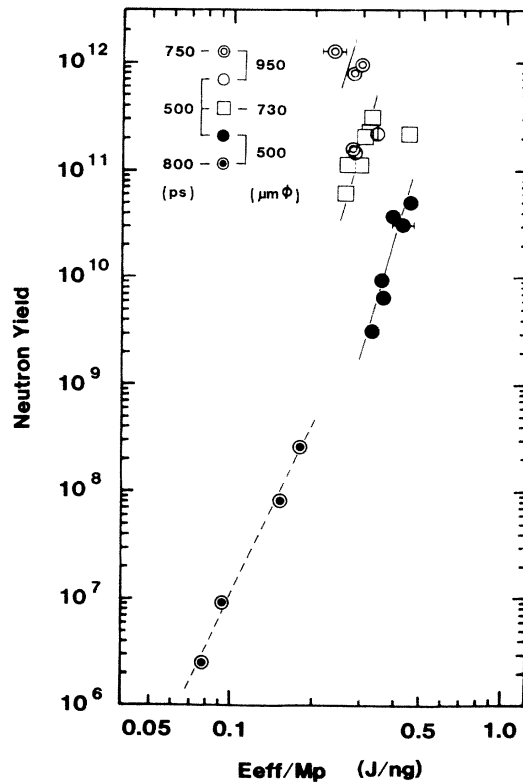


FIG. 2. Measured neutron-yield dependence on the specific energy. The highest neutron yield is seen for a 950- $\mu\text{m}$ -diam target with a 750-psec pulse.

high-aspect-ratio target is suitable for this purpose because the shell can be accelerated for a long distance up to a high velocity, resulting in a high neutron yield. Furthermore, a tailored pulse should be used to attain the shock multiplexing. However, we found by means of the simulation that a Gaussian pulse is good enough for this purpose; only the first half of the Gaussian pulse is used instead of the tailored pulse, with sacrifice of the rear half.

Figure 1(b) shows isointensity contours of an x-ray streak image from the target in EXP-B which produced the highest neutron yield. In contrast with the image in Fig. 1(a), the implosion mode matches with the Gaussian pulse. Figure 2 shows the neutron-yield dependence on the specific laser energy (the effective laser energy per unit pusher mass). The effective energies here were estimated under the assumption that the absorbed energies were effectively used until the target radius became  $\frac{1}{3}$  of the initial radius. The observed absorption rates were 40%–70% depending on the laser intensity. For the larger targets, a higher neutron yield was achieved. The targets of  $\sim 950\text{-}\mu\text{m}$  diameter were irradiated with both 500- and 750-psec pulses. The former cases (950  $\mu\text{m}$ , 500 psec) are seen to lie on the same curve in the figure as the  $\sim 730\text{-}\mu\text{m}$

TABLE I. Physical quantities obtained in the experiments, as in Fig. 1(b), compared with the simulation. The second row shows the simulation results given by the assumption of  $f_c = 0.03$  with a nonlocal treatment of tail electrons by the multigroup model.

	$T_i$ (fuel) (keV)	$T_e$ (fuel) (keV)	Absorption (%)	Neutron yield	Minimum core radius ( $\mu\text{m}$ )	$\rho$ (fuel) ( $\text{g}/\text{cm}^3$ )
Experiment	6.6–8.6	>1.79	$51.9 \pm 18.5$	$1.25 \times 10^{12}$	100	0.29
Simulation	7.02	2.62	63.3	$6.29 \times 10^{12}$	84	0.74

$\mu\text{m}$  targets. This represents the mismatch of the 500-psec laser pulse with the 950- $\mu\text{m}$  targets. In contrast, for the 750-psec pulse, higher neutron yields of up to  $1.25 \times 10^{12}$  were achieved at the same specific energies as those for 730- and 500- $\mu\text{m}$  targets.

From the above considerations, solutions for higher hydrodynamic efficiency and neutron yield are as follows: (1) Use a large-aspect-ratio target and accelerate the pusher wall to a high velocity for long duration; (2) shock-wave multiplexing is important, so that the first half of the Gaussian laser pulse must be synchronized with the pusher acceleration phase. Furthermore, it should be pointed out that even the thin shell used here was not burned through although the initial thickness of the shell is thinner than the burnthrough thickness deduced from the experimental scaling of the mass ablation rate for nonimploded targets.<sup>12,13</sup> This suggests that the shell is ablatively driven towards the center, increasing the pusher  $\rho R$  during the implosion. Actually, the simulation shows this increase of  $\rho R$  as depicted in Fig. 1. Furthermore, as seen from Fig. 1(b), the shock wave and the pusher arrived simultaneously at the center. These two facts suggest that shock-wave multiplexing surely occurred, because otherwise the pusher could not have caught up with the first shock wave.

A detailed comparison between the experiment and the simulation is made in Table I. In the second row are shown the simulation data with a flux limitation factor of 0.03 using the multigroup diffusion scheme in the thermal tail.<sup>14</sup> They are in good agreement.

One-dimensional spatially resolved x-ray spectroscopic measurements showed no pusher-fuel mixing in spite of the high aspect ratios of the targets. This fact is supported by the x-ray images of compressed core, where sphericity was better than 30%. It has been commonly recognized that the stagnation with a rapid deceleration is more stable than that with a slow deceleration because the surface perturbation  $\delta X$  is approximately given by  $\delta X = gt^2/2 = V^2/2g$  in the nonlinear phase. Here,  $V (=gt)$  is the implosion velocity and  $g$  the deceleration at the stagnation phase. Actually, the linear perturbation code<sup>10</sup> suggested that the implosion mode in EXP-B is more stable than that in EXP-A during the stagnation phase, whereas the form-

er is more unstable during the acceleration phase. Then the experimental results imply that there exists some mechanism to stabilize the Rayleigh-Taylor instability during the acceleration phase. The possible mechanisms which stabilize the implosion may be the decrease of the aspect ratio during the implosion and the Atwood number around the ablation region. The flow patterns obtained by the code HIMICO show the above effect.

In conclusion, we achieved the highest neutron yield ever measured,  $1.25 \times 10^{12}$ , with the GEKKO XII green-laser system. The implosion mode utilized shock-wave multiplexing with a quasitailored pulse in the first half of a Gaussian pulse. The implosion mode is close to an ablative mode because the matching between the implosion time and the laser pulse is one of the key issues and higher neutron yield was achieved for thinner targets.

In this shock-wave-multiplexing scheme, the pusher is always accelerated until the final stagnation. There is no to-and-fro motion between the core and the pusher due to the reflecting shock waves; this means that there is no mixing of the fuel. The neutron yield is well accounted for by the implosion simulation result. Experiments with these thin-walled, large-diameter shell targets give considerable insight into the characteristics of the implosion.

The authors are greatly indebted to K. Nishihara, S. Ido, and the students who joined these experiments for their contributions, and K. A. Tanaka and R. Stapf for valuable discussions.

<sup>1</sup>C. Yamanaka *et al.*, in *Proceedings of the Tenth International Conference on Plasma Physics and Controlled Nuclear Fusion Research, London, September 1984* (International Atomic Energy Agency, Vienna, 1985), IAEA-BI-1.

<sup>2</sup>R. G. Evans *et al.*, in Ref. 1, IAEA-BI-3.

<sup>3</sup>R. L. McCrory *et al.*, in Ref. 1, IAEA-BI-4-1.

<sup>4</sup>M. Nakatsuka *et al.*, Institute of Laser Engineering, Osaka University, Quarterly Progress Report No. ILE-QPR-84-8, 1984 (unpublished).

<sup>5</sup>R. E. Kidder, *Nucl. Fusion* **14**, 53 (1974); S. D. Bertke and E. B. Goldman, *Nucl. Fusion* **18**, 509 (1978).

<sup>6</sup>H. Nishimura *et al.*, *Rev. Sci. Instrum.* **56**, 1128 (1985).

<sup>7</sup>Y. Yabe *et al.*, Nucl. Fusion **21**, 803 (1981); S. Kiyokawa, T. Yabe, and T. Mochizuki, Jpn. J. Appl. Phys., Pt. 2 **22**, L772 (1983).

<sup>8</sup>S. Sakabe *et al.*, Jpn. J. Appl. Phys., Pt. 1 **23**, 460 (1984).

<sup>9</sup>J. R. Freeman, M. J. Clauser, and S. L. Thompson, Nucl. Fusion **17**, 223 (1977).

<sup>10</sup>F. Hattori, H. Takabe, and K. Mima, to be published.

<sup>11</sup>J. Nuckolls *et al.*, Nature (London) **239**, 139 (1972).

<sup>12</sup>N. Miyanaga, Institute of Laser Engineering, Osaka University, Quarterly Progress Report No. ILE-QPR-84-12,

1985 (unpublished).

<sup>13</sup>M. Nakai *et al.*, Institute of Laser Engineering, Osaka University, Research Report No. ILE-8513P, 1985 (to be published).

<sup>14</sup>J. F. Luciani, P. Mora, and J. Virmont, Phys. Rev. Lett. **51**, 1664 (1983); J. F. Luciani, P. Mora, and R. Pellat, Phys. Fluids **28**, 835 (1985); A. R. Bell, R. G. Evans, and D. J. Nicholas, Phys. Rev. Lett. **46**, 243 (1981); K. Kishimoto and K. Mima, J. Phys. Soc. Jpn. **52**, 3389 (1983).

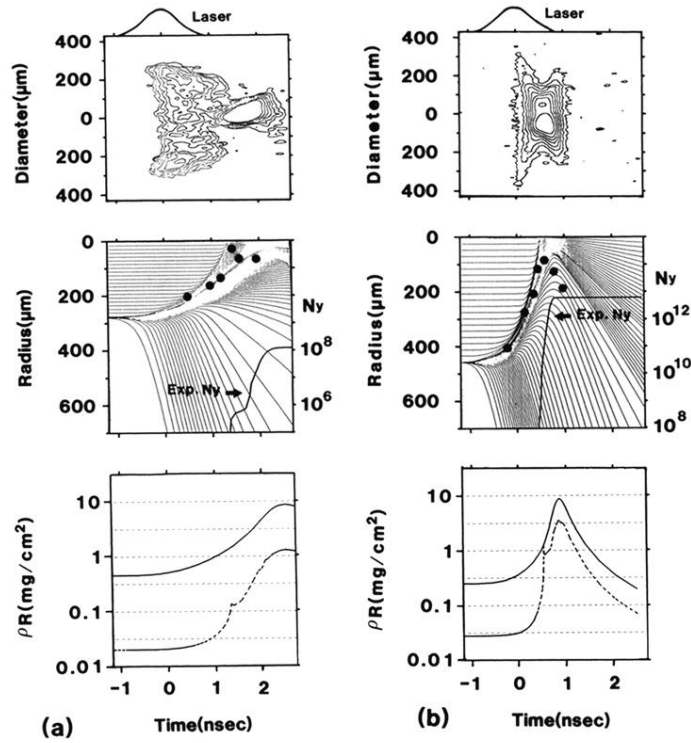


FIG. 1. (Bottom) Time evolution of  $\rho R$ , where the solid and the dashed lines represent the  $\rho R$  of the pusher and the fuel, respectively. (Middle) Flow diagrams and time-integrated neutron yields obtained by computer simulations. The experimental neutron yields are indicated by arrows. (Top) Isointensity contours of x-ray streak images of corresponding target shots. (a) 3.6-atm-DT-filled GMB of 545  $\mu\text{m}$  diam, 1.82  $\mu\text{m}$  thickness, coated with 3.6- $\mu\text{m}$ -thick CH, irradiated by 756 J per 800 psec at 0.53  $\mu\text{m}$  (EXP-A). (b) 3.0-atm-DT-filled GMB of 911  $\mu\text{m}$  diam, 1.46  $\mu\text{m}$  thickness, irradiated by 8045 J per 750 psec at 0.53  $\mu\text{m}$  (EXP-B).